Mean-Square Radius of Gyration and Second Virial Coefficient of Poly(diisopropyl fumarate) in Dilute Solution

By Masayuki NAKATSUJI, Munehiro HYAKUTAKE, Masashi OSA, and Takenao YOSHIZAKI[*]

The mean-square radius of gyration $\langle S^2 \rangle$ and second virial coefficient A_2 were determined from light scattering measurements for 13 samples of poly(diisopropyl fumarate) (PDiPF), each with the fraction of racemo diads $f_r = 0.22$, in a range of weight-average molecular weight from 4.02×10^4 to 8.59×10^5 in tetrahydrofuran at 30.0 °C. From a simultaneous analysis of the present data for $\langle S^2 \rangle$ and A_2 on the basis of the Kratky–Porod (KP) wormlike chain with excluded volume, the KP model parameters for PDiPF, i.e., the stiffness parameter λ^{-1} and the shift factor M_L are determined to be 113 Å and 89 Å^{-1}, respectively, the M_L value being consistent with that estimated on the basis of chain conformations of PDiPF. The λ^{-1} value indicates that PDiPF is stiffer than typical flexible polymers but not so stiff as typical semiflexible polymers such as poly(n-hexyl isocyanate).

KEY WORDS: Poly(diisopropyl fumarate) / Mean-Square Radius of Gyration / Second Virial Coefficient / Semiflexible Polymer / Kratky–Porod Wormlike Chain / Excluded-Volume Effect /

About 30 years ago, Bengough et al.[1] and Otsu et al.[2–5] found that dialkyl fumarate (DRF) such as isopropyl fumarate can polymerize to yield poly(DRF) through radical polymerization. Because of steric hindrances to internal rotations caused by substituents on every main-chain carbon atom, poly(DRF) chains were considered to be stiffer than familiar vinyl polymer chains having substituents on every other main-chain carbon atom. Subsequently, Matsumoto and Nakagawa[6] confirmed the conjecture by an analysis of experimental data for the intrinsic viscosity of poly(diisopropyl fumarate) (PDiPF) in tetrahydrofuran (THF) at 30.0 °C on the basis of the Kratky–Porod (KP) wormlike chain model.[7,8] The value of the stiffness parameter λ^{-1} for PDiPF was determined to be 220 Å, which is appreciably larger than those for typical flexible polymers such as atactic polystyrene (a-PS) ($\lambda^{-1} = 20._6$ Å)[8,9] or atactic poly(methyl methacrylate) (a-PMMA) ($\lambda^{-1} = 57._9$ Å).[8,10]

In the above analysis, Matsumoto and Nakagawa assumed that the intramolecular excluded-volume effect was negligibly small if any, although THF is a good solvent for PDiPF. The effect may actually be ignored for a semiflexible polymer if its λ^{-1} is very large and its molecular weight M (chain length) is not very large, as in the case of poly(n-hexyl isocyanate) (PHIC) whose λ^{-1} is 840 Å.[11] The λ^{-1} value 220 Å determined for PDiPF is, however, not so large as that for PHIC. Further, in a recent study of dilute solution properties of cellulose tris(phenyl carbamate) (CTC) made by Kasabo et al.,[12] it has been shown that the intramolecular excluded-volume effect cannot be ignored even for a polymer with $\lambda^{-1} = 210$ Å in an ordinary range of M. In order to evaluate λ^{-1} accurately for PDiPF, therefore, it is desirable to make an analysis with due consideration of the excluded-volume effects. This is the purpose of the present paper.

The determination of λ^{-1} for PDiPF in a good solvent requires some comments. We could determine it from an analysis only of the mean-square radius of gyration $\langle S^2 \rangle$ as a function of the weight-average molecular weight M_w by the use of the method proposed by Murakami et al.,[11] if experimental data were obtained for $\langle S^2 \rangle$ in an M_w range where the intramolecular excluded-volume effect might be ignored. In anticipation of results, we note that the effect on $\langle S^2 \rangle$ cannot be ignored in the whole range of M_w ($4.02 \times 10^4 \leq M_w \leq 8.59 \times 10^5$) examined. Then we make a maiden attempt to analyze $\langle S^2 \rangle$ and the second virial coefficient A_2 simultaneously, both determined from light scattering (LS) measurements, on the basis of the quasi-two-parameter (QTP) scheme[8,13–15] for the intramolecular excluded-volume effect and also the Yamakawa theory[8,16] of A_2 which is concerned with the intermolecular one.

EXPERIMENTAL

Materials

Three original PDiPF samples were synthesized by radical polymerization, following the procedure of Otsu et al.[4,5] and Matsumoto and Nakagawa.[6] Polymerization was carried out in benzene by the use of dimethyl 2,2′-azobis(isobutyrate) as an initiator under dry nitrogen at 60 °C for ca. 120 h for two samples in the range of $M_w \lesssim 4 \times 10^5$ and under a high vacuum condition at 40 °C for ca. 240 h for the other sample having larger M_w. It was terminated by pouring each polymerization mixture into a large amount of hexane to precipitate an original sample. Each original sample so synthesized was separated into fractions by fractional precipitation using benzene as a solvent and methanol as a precipitant. 13 test samples so obtained were freeze-dried from their benzene solutions after filtration through a Teflon membrane of pore size 1.0 μm.

Department of Polymer Chemistry, Kyoto University, Katsura, Kyoto 615-8510, Japan
[*]To whom correspondence should be addressed (E-mail: yoshizaki@molsci.polym.kyoto-u.ac.jp).

The values of the ratio of M_w to the number-average molecular weight M_n for all the samples except the two having the smallest and largest M_w were determined from analytical gel permeation chromatography (GPC) using tetrahydrofuran as an eluent.

The solvent THF used for LS was purified by distillation after refluxing over sodium. The solvents THF and deuterated chloroform used for analytical GPC and ^{13}C NMR spectroscopy, respectively, were of reagent grade.

Light Scattering

LS measurements were carried out to determine M_w and A_2 for all the 13 test samples and $\langle S^2 \rangle$ for 10 test samples with $M_w \gtrsim 8 \times 10^4$, in THF at 30.0 °C. A Fica 50 light-scattering photometer was used for all the measurements with vertically polarized incident light of wavelength $\lambda_0 = 436$ nm. For a calibration of the apparatus, the intensity of light scattered from pure benzene was measured at 25.0 °C at a scattering angle of 90°, where the Rayleigh ratio $R_{Uu}(90°)$ of pure benzene was taken as 46.5×10^{-6} cm^{-1}.[17] The depolarization ratio ρ_u of pure benzene at 25.0 °C was determined to be 0.41 ± 0.01. Scattered intensity was measured at six different concentrations and at scattering angles θ ranging from 30.0 to 142.5°. The data obtained were treated by using the Berry square-root plot.[18] For three samples with $M_w \lesssim 7 \times 10^4$, corrections for optical anisotropy were necessary to estimate the true M_w and A_2. Therefore, the excess depolarized (Hv) components ΔR_{Hv} of the reduced scattered intensity for their solutions were measured in addition to the excess unpolarized (Uv) components ΔR_{Uv} in order to make those necessary corrections. As for the other samples with $M_w \gtrsim 8 \times 10^4$, effects of optical anisotropy were negligibly small, so that the corrections were unnecessary and only ΔR_{Uv} was measured for each solution.

The most concentrated solution of each sample was prepared gravimetrically and made homogeneous by continuous stirring in the dark at room temperature for 2 d. It was optically purified by filtration through a Teflon membrane of pore size 0.45 or 0.10 μm. The solutions of lower concentrations were obtained by successive dilution. The weight concentrations were converted to the polymer mass concentrations c by the use of the densities of the respective solutions calculated with the partial specific volumes v_2 of the samples and with the density ρ_0 of the solvent THF. The quantities v_2 and ρ_0 were measured with a pycnometer of the Lipkin–Davison type having a volume of 3 cm^3. The values of v_2 so determined in THF at 30.0 °C are 0.873 cm^3/g for all the samples independently of M_w. The value of ρ_0 of THF at 30.0 °C is 0.8751 g/cm^3.

The refractive index increment $\partial n/\partial c$ was measured at the wavelength of 436 nm by the use of a Shimadzu differential refractometer. The values of $\partial n/\partial c$ so determined in THF at 30.0 °C are 0.0623$_3$ cm^3/g for all the samples independently of M_w. The value of the refractive index n_0 of THF at 30.0 °C and at the wavelength of 436 nm was determined to be 1.410$_8$ by the use of an Abbe refractometer (ERMA OPTICAL WORKS).

^{13}C NMR

^{13}C NMR spectra for three of the 13 test samples and for the (unfractionated) three original samples were recorded on a JEOL JNM EX-400 spectrometer at 100.4 MHz. The spectra were taken in deuterated chloroform at room temperature using an rf pulse angle of 90° with a pulse repetition time of 3 s. The relative chemical shifts δ_r of ^{13}C signals of a test sample referred to the ^{13}C signal of chloroform were measured and then converted to the chemical shifts in the tetramethylsilane scale $\delta = \delta_r + 77.00$ ppm.

RESULTS

As is well known, we cannot correctly evaluate M_w, $\langle S^2 \rangle$, and A_2 from the (standard) Berry square-root plot if the effects of optical anisotropy of polymer chains are not small,[19–23] and must make an appropriate correction for the optical anisotropy. Following the standard procedure[19–23] by the use of the reduced Hv component ΔR_{Hv} of the excess scattered intensity in addition to the Uv component ΔR_{Uv} used for the square-root plot, we may calculate M_w and the optical anisotropy factor δ from

$$\lim_{c,\theta \to 0} \frac{\Delta R_{Uv}}{2Kc} = M_{w,ap} = (1 + 7\delta)M_w \qquad (1)$$

$$\lim_{c,\theta \to 0} \frac{\Delta R_{Hv}}{2Kc} = 3\delta M_w \qquad (2)$$

with the values of $\Delta R_{Uv}/2Kc$ and $\Delta R_{Hv}/2Kc$ in the limit of the vanishing mass concentration c and scattering angle θ. In eqs 1 and 2, K is the optical constant and $M_{w,ap}$ is the the apparent weight-average molecular weight determined directly from the square-root plot. In the second and third columns of Table I are given the values of M_w and δ so determined for all the 13 samples. We note that the correction for the optical anisotropy is not necessary for the samples PDiPF8 through PDiPF86.

For the three samples PDiPF4, PDiPF5, and PDiPF6, the apparent mean-square radius of gyration $\langle S^2 \rangle_{ap}$ could not be evaluated directly from the square-root plot with sufficient accuracy to estimate (true) $\langle S^2 \rangle$, because the slopes of the plots are very small for these samples. As for the other 10 samples with larger M_w, for which correction for the optical anisotropy is unnecessary, $\langle S^2 \rangle$ for each sample may be equated to $\langle S^2 \rangle_{ap}$

Table I. Experimental Results for Poly(diisopropyl fumarate)

sample	M_w	$10^3\delta$	$10^{-4}\langle S^2 \rangle$ (Å^2)	$10^4 A_2$ (cm^3 mol/g^2)	M_w/M_n	f_r
PDiPF4	4.02×10^4	9.1$_2$		5.1$_4$		
PDiPF5	4.95×10^4	8.8$_6$		5.4$_5$	1.10	0.22
PDiPF6	6.31×10^4	5.2$_0$		4.9$_3$	1.05	
PDiPF8	8.00×10^4		1.4$_2$	4.2$_5$	1.10	
PDiPF9	9.17×10^4		1.7$_9$	4.0$_7$	1.07	
PDiPF15	1.53×10^5		3.1$_9$	4.0$_0$	1.08	
PDiPF18	1.83×10^5		3.9$_1$	3.5$_1$	1.08	0.22
PDiPF22	2.18×10^5		5.0$_3$	3.7$_5$	1.09	
PDiPF34	3.37×10^5		7.9$_8$	3.5$_3$	1.07	
PDiPF44	4.37×10^5		10.8	3.4$_5$	1.07	
PDiPF50	5.00×10^5		11.8	3.3$_4$	1.05	0.22
PDiPF62	6.20×10^5		15.3	2.9$_1$	1.05	
PDiPF86	8.59×10^5		20.9	2.9$_9$		

evaluated directly from the slope of the plot. The values of $\langle S^2 \rangle$ so determined for the 10 samples are given in the fourth column of Table I.

The correction for the optical anisotropy to A_2 may be given by[19-21]

$$A_{2,\text{ap}} = A_2 (1 + 7\delta)^{-2} \qquad (3)$$

For the three samples PDiPF4, PDiPF5, and PDiPF6, the values of A_2 have been calculated from eq 3 with the values of δ given in the third column of Table I and also the values of the apparent second virial coefficient $A_{2,\text{ap}}$ determined directly from the square-root plot. As for the other 10 samples with larger M_w, for which the correction for the optical anisotropy is unnecessary, A_2 for each sample may be equated to $A_{2,\text{ap}}$. The values of A_2 so determined for all the samples are given in the fifth column of Table I.

In the sixth column of Table I are also given the values of the ratio of M_w to M_n determined for all the samples except PDiPF4 and PDiPF86 by analytical GPC with the use of the values of M_w of all the samples given in the second column of the table. It is seen that the samples PDiPF5 through PDiPF62 are very narrow in molecular weight distribution. Although M_w/M_n could not be evaluated for the samples PDiPF4 and PDiPF86 with high accuracy because of lack of the calibration curve in the necessary range, their molecular weight distribution may be considered to be as narrow as that of the other samples.

From intensity of signals in the ^{13}C NMR spectra in a range of the chemical shift from 40.0 to 50.0 ppm, we have determined stereochemical compositions of the three samples PDiPF5, PDiPF18, and PDiPF50 and also of the (unfractionated) three original samples. Naturally, stereochemical terminology used for PDiPF composed of successive (pseudo-)-asymmetric backbone carbon atoms is different from that for vinyl polymers in which every other backbone carbon atoms are asymmetric. Following the terminology proposed by Wang *et al.*,[24] we call a pair of adjacent backbone carbon atoms (diad) in a PDiPF chain *meso* if vicinal substituents joined to them are located on opposite sides of a plane containing all the backbone carbon atoms of the PDiPF chain in the planar *trans* conformation, and *racemo* otherwise. According to Wang *et al.*[24] and Yoshioka *et al.*,[25] the signals in the above range of the chemical shift may then be assigned to the *meso* and *racemo* diads. The stereochemical compositions specified by fractions f_r of *racemo* diads for the test samples PDiPF5, PDiPF18, and PDiPF50 are given in the last column of Table I, which are consistent with the literature values[24,25] 0.22–0.23. The values of f_r for the original samples are the same as those for the three test samples, indicating that all the PDiPF samples should have the same value 0.22 of f_r.

Figure 1 shows double-logarithmic plots of $\langle S^2 \rangle / M_w$ ($\langle S^2 \rangle$ in Å^2) against M_w for PDiPF in THF at 30.0 °C. The unfilled circles represent the present experimental data. The solid and dashed curves represent the theoretical values for the KP chain with and without excluded volume, respectively, which are obtained and discussed in the next (DISCUSSION) section. It is seen that $\langle S^2 \rangle / M_w$ increases monotonically with increasing
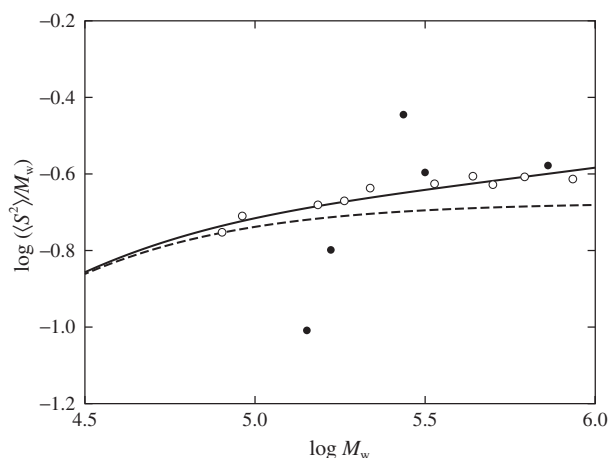
Figure 1. Double-logarithmic plots of $\langle S^2 \rangle / M_w$ ($\langle S^2 \rangle$ in Å^2) against M_w for PDiPF in THF at 30.0 °C: (○) present data; (●) data by Matsumoto and Nakagawa.[6] The solid and dashed curves represent the best-fit theoretical values for the KP chain with and without excluded volume.
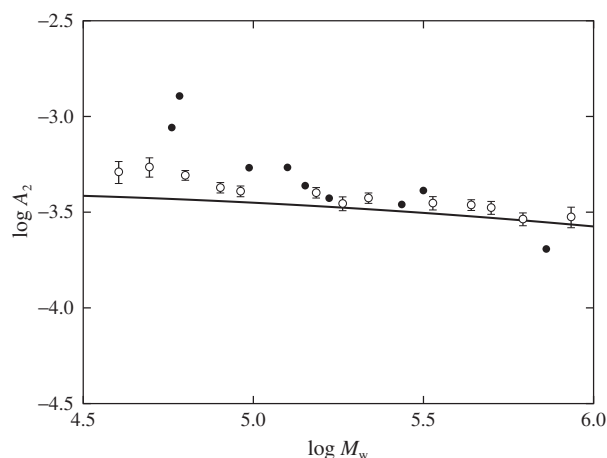
Figure 2. Double-logarithmic plots of A_2 (in cm^3 mol/g^2) against M_w for PDiPF in THF at 30.0 °C. All the symbols have the same meaning as those in Figure 1. The vertical line segments attached to the present data points (○) indicate the error bounds. The solid curve represents the theoretical values for the KP chain without the effects of chain ends (see the text).

M_w. It is also seen that the present data points form a curve convex upward, the slope of which is *ca.* 0.19 for $M_w \lesssim 2 \times 10^5$ and *ca.* 0.08 for $M_w \gtrsim 3 \times 10^5$. The rather steep slope in the range of $M_w \lesssim 2 \times 10^5$ may be due to effects of chain stiffness of PDiPF. For comparison, literature data for PDiPF in THF at 30.0 °C by Matsumoto and Nakagawa[6] are also plotted in the figure (filled circles). Their values are scattered around ours in the range of $M_w \lesssim 3 \times 10^5$ but agree with ours within experimental error in the range of $M_w \gtrsim 3 \times 10^5$.

Figure 2 shows double-logarithmic plots of A_2 (in cm^3 mol/ g^2) against M_w for PDiPF in THF at 30.0 °C. All the symbols have the same meaning as those in Figure 1. The vertical line segment attached to each present data point (○) indicates its error bound. The solid curve represents the theoretical values for the KP chain without effects of chain ends, which are

obtained and discussed in the next (DISCUSSION) section. The present data points follow a straight line of slope *ca.* -0.13, which is appreciably larger than *ca.* -0.2 for typical flexible polymers with large M_w in good solvents, implying that the PDiPF chain has rather large stiffness. The literature data obtained by Matsumoto and Nakagawa[6] (filled circles) agree well with the present ones, although they are somewhat scattered in the range of $M_w \lesssim 1 \times 10^5$.

DISCUSSION

Now we proceed to analyze the present data for $⟨S^2⟩$ and A_2 for PDiPF given in the last section on the basis of the KP theory of the unperturbed mean-square radius of gyration[8,26] $⟨S^2⟩_0$ along with the QTP scheme or the Yamakawa–Stockmayer–Shimada theory[8,13–15] of the intramolecular excluded-volume effect and also of the Yamakawa theory[8,16] of A_2.

For the KP chain of total contour length L, $⟨S^2⟩$ may be written in the form,

$$⟨S^2⟩ = ⟨S^2⟩_0 \, \alpha_S^2 \tag{4}$$

where $⟨S^2⟩_0$ is given by[8,26]

$$⟨S^2⟩_0 = \frac{L}{6\lambda} - \frac{1}{4\lambda^2} + \frac{1}{4\lambda^3 L} - \frac{1}{8\lambda^4 L^2}(1 - e^{-2\lambda L}) \tag{5}$$

and the gyration-radius expansion factor α_S may be given by the Domb–Barrett equation,[27]

$$\begin{aligned} \alpha_S^2 = &[1 + 10\tilde{z} + (\tfrac{70\pi}{9} + \tfrac{10}{3})\tilde{z}^2 + 8\pi^{3/2}\tilde{z}^3]^{2/15} \\ &\times [0.933 + 0.067\exp(-0.85\tilde{z} - 1.39\tilde{z}^2)] \end{aligned} \tag{6}$$

In the QTP scheme, the (conventional) excluded-volume parameter z defined in the two-parameter (TP) scheme on the basis of the Gaussian chain model is replaced by the intramolecular scaled excluded-volume parameter $\tilde{z}$ defined by

$$\tilde{z} = \frac{3}{4}K(\lambda L)z \tag{7}$$

where the coefficient $K(\lambda L)$ as a function of the reduced contour length λL is given by

$$\begin{aligned} K(\lambda L) = &\tfrac{4}{3} - 2.711(\lambda L)^{-1/2} + \tfrac{7}{6}(\lambda L)^{-1} \quad \text{for } \lambda L > 6 \\ = &(\lambda L)^{-1/2}\exp[-6.611(\lambda L)^{-1} \\ &+ 0.9198 + 0.03516\lambda L] \qquad \text{for } \lambda L \leq 6 \end{aligned} \tag{8}$$

The quantity $K(\lambda L)$ represents the effects of chain stiffness on the intramolecular excluded-volume effect or on the intramolecular contact probability and increases monotonically from 0 to 4/3 as λL is increased from 0 to ∞. Then, in the limit of $\lambda L \to \infty$ (random-coil limit) the QTP scheme reduces to the

TP one, *i.e.*, $\tilde{z} = z$, while in the limit of $\lambda L \to 0$ (rod limit) $\tilde{z}$ vanishes irrespective of the value of z.

The QTP scheme is formulated on the basis of a model composed of $n + 1$ beads of the binary-cluster integral β arrayed with spacing a between them along the KP or helical wormlike (HW) chain[8] of total contour length L, so that $L = na$. The parameter z may then be written in terms of β, a, and λL as

$$z = (3/2\pi)^{3/2}(\lambda B)(\lambda L)^{1/2} \tag{9}$$

where B is the excluded-volume strength defined by

$$B = \beta/a^2 c_\infty^{3/2} \tag{10}$$

with

$$c_\infty = \lim_{\lambda L \to \infty}(6\lambda⟨S^2⟩_0/L) \tag{11}$$

As seen from eq 11 with eq 5, c_∞ is equal to unity for the KP chain.

In the Yamakawa theory[8,16] of A_2, effects of chain stiffness and chain ends are taken into account, and A_2 may then be written in the form,

$$A_2 = A_2^{(HW)} + A_2^{(E)} \tag{12}$$

where $A_2^{(HW)}$ is a part of A_2 without the effects of chain ends and $A_2^{(E)}$ represents contribution of the effects of chain ends to A_2. The superscript (HW) attached to the first term indicates that the theory is formulated on the basis of the HW chain, and the following theoretical expression for $A_2^{(HW)}$ reduces to that for the KP chain if c_∞ is set equal to unity.

For the KP (or HW) chain of total contour length L with the excluded-volume strength B, $A_2^{(HW)}$ may be given by

$$A_2^{(HW)} = (N_A c_\infty^{3/2} L^2 B/2M^2)h(\hat{z}) \tag{13}$$

where N_A is the Avogadro constant, M is the polymer molecular weight, and h is given by

$$h(\hat{z}) = (1 + 7.74\hat{z} + 52.3\hat{z}^{27/10})^{-10/27} \tag{14}$$

with

$$\hat{z} = \tilde{z}/\alpha_S^3 \tag{15}$$

In eq 15, $\tilde{z}$ is the intermolecular scaled excluded-volume parameter defined by

$$\tilde{z} = \left[\frac{Q(\lambda L)}{2.865}\right]z \tag{16}$$

The coefficient $Q(\lambda L)$ in eq 16 as a function of λL represents the effects of chain stiffness on the intermolecular excluded-volume effect and is given in a very good approximation for $\lambda L \gtrsim 1$ by[8,16]

$$\begin{aligned} Q(\lambda L) = &-\tfrac{128\sqrt{2}}{15} - 2.531(\lambda L)^{-1/2} - 2.586(\lambda L)^{-1} + 1.985(\lambda L)^{-3/2} \\ &- 1.984(\lambda L)^{-2} - 0.9292(\lambda L)^{-5/2} + 0.1223(\lambda L)^{-3} + \tfrac{8}{5}x^{5/2} \\ &+ \tfrac{2}{3}x^{3/2}[8 + \tfrac{1}{6}(\lambda L)^{-1}] + x^{1/2}[8 - 13.53(\lambda L)^{-1} + 0.2804(\lambda L)^{-2}] \\ &- x^{-1/2}(\lambda L)^{-1}[0.3333 - 5.724(\lambda L)^{-1} + 0.7974(\lambda L)^{-2}] \\ &- x^{-3/2}(\lambda L)^{-2}[0.3398 - 0.7146(\lambda L)^{-1}] \end{aligned} \tag{17}$$

with

$$x = 1 + 0.961(\lambda L)^{-1} \tag{18}$$

It is seen from eq 16 with eqs 17 and 18 that $\tilde{\tilde{z}}$ becomes identical with z in the limit of $\lambda L \to \infty$ as in the case of $\tilde{z}$ and therefore $A_2^{(HW)}$ reduces to A_2 given by the TP theory.

As for the second term $A_2^{(E)}$ in eq 12, we omit its detailed expression[8,16] since it is not necessary for the present analysis of A_2. We only note that $A_2^{(E)}$ rapidly decreases to 0 with increasing M and may be neglected for $M \gtrsim 10^5$ for all the polymer-solvent systems examined so far.[8,12,28–31]

In order to compare the above-mentioned KP theoretical values of $\langle S^2 \rangle$ and A_2 as functions of L with the experimental ones as functions of M, L is related to M by

$$L = M/M_L \tag{19}$$

where M_L is the shift factor as defined as the molecular weight per unit contour length of the KP (or HW) chain. We may then determine the three parameters λ^{-1}, M_L, and λB by the curve fitting to the experimental data for $\langle S^2 \rangle$ or A_2. As already mentioned, we cannot determine them only from the data for $\langle S^2 \rangle$, so that we attempt to carry out the curve fitting to both the data for $\langle S^2 \rangle$ and A_2 simultaneously.

In Figures 1 and 2, the solid curves represent the best-fit KP theory values of $\langle S^2 \rangle$ and those of A_2 without consideration of the effects of chain ends ($A_2^{(E)} = 0$), respectively, where the former values have been calculated from eq 4 with eqs 5–9 and 19 and the latter from eq 12 with eqs 6–9 and 13–19, with $\lambda^{-1} = 113$ Å, $M_L = 89$ Å^{-1}, and $\lambda B = 0.097$. We note that relative errors in those parameter values are 8, 5, and 10%, respectively, at most. It is seen from the figures that the theoretical values of $\langle S^2 \rangle$ quantitatively reproduce the experimental ones over the whole range of M_w examined and the theoretical values of A_2 ($= A_2^{(HW)}$) may rather well reproduce the experimental ones within experimental error in the range of $M_w \gtrsim 10^5$, where the effects of chain ends may be neglected. In Figure 2, the present data points deviate upward progressively from the theoretical curve with decreasing M_w for $M_w \lesssim 10^5$. It may be regarded as arising from the effects of chain ends ($A_2^{(E)} = 0$). From an analysis of the difference between the observed A_2 and the theoretical $A_2^{(HW)}$, we may obtain information about the excess (effective) binary-cluster integrals of terminal beads.[8,16] Such an analysis is beyond the scope of the present work, and we do not pursue further it.

In Figure 1 are also shown the theoretical values of $\langle S^2 \rangle_0$ (dashed curve) calculated from eq 5 with the values of λ^{-1} and M_L determined above. It is seen that the present data points deviate upward progressively from the theoretical $\langle S^2 \rangle_0$ with increasing M_w due to the intramolecular excluded-volume effect.

Finally, it is interesting to analyze the present data for $\langle S^2 \rangle$ shown in Figure 1 on the basis of the KP chain without excluded volume, as considered by Matsumoto and Nakagawa.[6] We have obtained $\lambda^{-1} = 154$ Å and $M_L = 103$ Å^{-1} from the curve fitting, although the best-fit unperturbed KP values of $\langle S^2 \rangle_0$ have been omitted in Figure 1, for simplicity.

top views

side views

○ : H
● : C
● : O

10Å

(a)   (b)   (c)
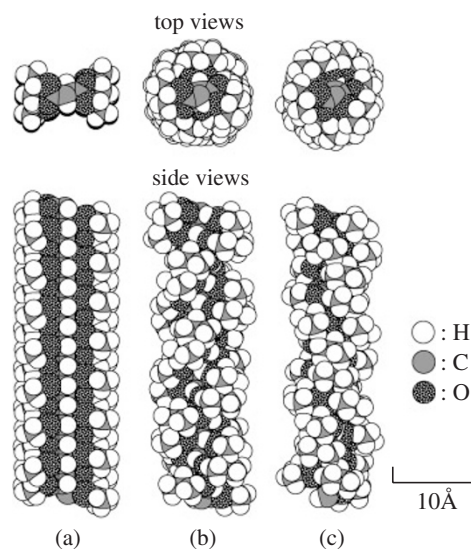
Figure 3. Schematic drawing of chain conformations of PDiPF with $f_r = 0$, where all atoms are depicted by the spheres having the van der Walls radii: (a) planar *trans* conformation with $\phi = 0$; (b) helical conformation with $\phi = 30°$; (c) helical conformation with $\phi = 60°$.

Note that the KP chain without excluded volume cannot explain the experimental data for A_2, needless to say. The value 89 Å^{-1} of M_L determined from the present analysis with consideration of the intra- and intermolecular excluded-volume effects is remarkably smaller than the above value 103 Å^{-1} and also the literature value 134 Å^{-1} by Matsumoto and Nakagawa, both without consideration of the intramolecular excluded-volume effects.

For the PDiPF chain (with $f_r = 0$) in the planar *trans* conformation (with a bond angle of 109°), which is schematically depicted in Figure 3(a), M_L may be evaluated to be 80.3 Å^{-1}. A polymer chain in a helical conformation in principle has an M_L value larger than that for the chain in the planar *trans* conformation, and therefore the (true) M_L value for the PDiPF chain seems larger than 80.3 Å^{-1}. For trial calculations of M_L for the PDiPF chain (with $f_r = 0$) in helical conformations, we consider two chains having fixed internal rotation angles $\phi = 30°$ and 60°, which are schematically depicted in Figure 3(b) and 3(c), respectively. Note that the chain with $\phi = 0°$ is in the planar *trans* conformation. The values of M_L are evaluated to be 81.3 and 84.7 Å^{-1} for $\phi = 30°$ and 60°, respectively, which are not very larger than 80.3 Å^{-1}. Considering this fact, the value 89 Å^{-1} of M_L seems reasonable, and analyses of data for PDiPF in THF at 30.0 °C without consideration of the excluded-volume effects lead to overestimation of the value of M_L and also that of λ^{-1}.

CONCLUDING REMARKS

We have carried out LS measurements to determine $\langle S^2 \rangle$ and A_2 for PDiPF in THF at 30.0 °C and then determined its KP model parameters λ^{-1} and M_L by analyzing the data so obtained on the basis of the corresponding KP (or HW) theories

with consideration of the intra- and intermolecular excluded-volume effects. The value 113 Å of λ^{-1} determined in the present analysis is smaller than 220 Å obtained by Matsumoto and Nakagawa[6] from an analysis of $[\eta]$ without consideration of the intramolecular excluded-volume effect. However, the qualitative characteristic of PDiPF proposed by them is still valid, *i.e.*, its chain stiffness is larger than that of typical flexible polymers such as a-PS and a-PMMA but not so large as that of typical semiflexible polymers such as PHIC. The value 89 Å^{-1} of M_L is also smaller than their value 134 Å^{-1}, the former value being consistent with that estimated on the basis of the chain conformations of PDiPF. It may then be said that analyses of data for PDiPF in THF at 30.0 °C without consideration of the excluded-volume effects lead to over-estimation of both the values of λ^{-1} and M_L.

In order to confirm the result of the present analysis of $\langle S^2 \rangle$ and A_2, it is desirable to make a study of steady-state transport coefficients such as $[\eta]$ and the translational diffusion coefficient of PDiPF. Thus we proceed to make such a study in a forthcoming paper.

REFERENCES

1. W. I. Bengough, G. B. Park, and R. A. Young, *Eur. Polym. J.*, **11**, 305 (1975).
2. T. Otsu, O. Ito, N. Toyoda, and S. Mori, *Makromol. Chem., Rapid Commun.*, **2**, 725 (1981).
3. T. Otsu, T. Yasuhara, K. Shiraishi, and S. Mori, *Polym. Bull.*, **12**, 449 (1984).
4. T. Otsu, H. Minai, N. Toyoda, and T. Yasuhara, *Makromol. Chem., Suppl.*, **12**, 133 (1985).
5. T. Otsu, T. Yasuhara, and A. Matsumoto, *J. Macromol. Sci. Chem.*, **A25**, 537 (1988).
6. A. Matsumoto and E. Nakagawa, *Eur. Polym. J.*, **35**, 2107 (1999).
7. O. Kratky and G. Porod, *Recl. Trav. Chim. Pays-Bas*, **68**, 1106 (1949).
8. H. Yamakawa, "Helical Wormlike Chains in Polymer Solutions," Springer, Berlin, 1997.
9. F. Abe, Y. Einaga, T. Yoshizaki, and H. Yamakawa, *Macromolecules*, **26**, 1884 (1993).
10. Y. Tamai, T. Konishi, Y. Einaga, M. Fujii, and H. Yamakawa, *Macromolecules*, **23**, 4067 (1990).
11. H. Murakami, T. Norisuye, and H. Fujita, *Macromolecules*, **13**, 345 (1980).
12. F. Kasabo, T. Kanematsu, T. Nakagawa, T. Sato, and A. Teramoto, *Macromolecules*, **33**, 2748 (2000).
13. H. Yamakawa and W. H. Stockmayer, *J. Chem. Phys.*, **57**, 2843 (1972).
14. H. Yamakawa and J. Shimada, *J. Chem. Phys.*, **83**, 2607 (1985).
15. J. Shimada and H. Yamakawa, *J. Chem. Phys.*, **85**, 591 (1986).
16. H. Yamakawa, *Macromolecules*, **25**, 1912 (1992).
17. Gj. Deželić and J. Vavra, *Croat. Chem. Acta*, **38**, 35 (1966).
18. G. C. Berry, *J. Chem. Phys.*, **44**, 4550 (1966).
19. H. Yamakawa, "Modern Theory of Polymer Solutions," Harper & Row, New York, 1971. Its electronic edition is available on-line at the URL: http://www.molsci.polym.kyoto-u.ac.jp/archives/redbook.pdf
20. H. Utiyama and M. Kurata, *Bull. Inst. Chem. Res. Kyoto Univ.*, **42**, 128 (1964).
21. H. Utiyama, *J. Phys. Chem.*, **69**, 4138 (1965).
22. K. Nagai, *Polym. J.*, **3**, 67 (1972).
23. H. Yamakawa, M. Fujii, and J. Shimada, *J. Chem. Phys.*, **71**, 1611 (1979).
24. X. Wang, T. Komoto, I. Ando, and T. Otsu, *Makromol. Chem.*, **189**, 1845 (1988).
25. M. Yoshioka, A. Matsumoto, and T. Otsu, *Polym. J.*, **23**, 1191 (1991).
26. H. Benoit and P. Doty, *J. Phys. Chem.*, **57**, 958 (1953).
27. C. Domb and A. J. Barrett, *Polymer*, **17**, 179 (1976).
28. Y. Einaga, F. Abe, and H. Yamakawa, *Macromolecules*, **26**, 6243 (1993).
29. F. Abe, Y. Einaga, and H. Yamakawa, *Macromolecules*, **27**, 3262 (1994).
30. M. Kamijo, F. Abe, Y. Einaga, and H. Yamakawa, *Macromolecules*, **28**, 4159 (1995).
31. W. Tokuhara, M. Osa, T. Yoshizaki, and H. Yamakawa, *Macromolecules*, **36**, 5311 (2003).